

Magnetic Anisotropy of Strained Epitaxial Manganite Films

V. V. Demidov^{a,*}, I. V. Borisenko^a, A. A. Klimov^a, G. A. Ovsyannikov^{a,b},
A. M. Petrzikh^a, and S. A. Nikitov^a

^a Institute of Radio-Engineering and Electronics, Russian Academy of Sciences, Moscow, 125009 Russia
e-mail: demidov@cplire.ru

^b Chalmers University of Technology, SE-41296, Gothenburg, Sweden

Received October 4, 2010

Abstract—The in-plane magnetic anisotropy of epitaxial $\text{La}_{0.7}\text{Sr}_{0.3}\text{MnO}_3$ (LSMO) films is studied at room temperature by the following three independent techniques: magneto-optical Kerr effect, ferromagnetic resonance at a frequency of 9.61 GHz, and recording of absorption spectra of electromagnetic radiation at a frequency of 290.6 MHz. The films are deposited onto NdGaO_3 (NGO) substrates in which the (110) NGO plane is tilted at an angle of 0–25.7° to the substrate plane. The uniaxial magnetic anisotropy induced by the strain of the film is found to increase with the tilt angle of the (110) NGO plane. A model is proposed to describe the change in the magnetic anisotropy energy with the tilt angle. A sharp increase in the radio-frequency absorption in a narrow angular range of a dc magnetic field near a hard magnetization axis is detected. The anisotropy parameters of the LSMO films grown on (110) NGO, (001) SrTiO_3 , and (001)[$(\text{LaAlO}_3)_{0.3} + (\text{Sr}_2\text{AlTaO}_6)_{0.7}$] substrates are compared.

DOI: 10.1134/S1063776111040029

1. INTRODUCTION

As was shown in [1–10], the electrical and magnetic parameters of epitaxial $\text{Re}_{1-x}\text{A}_x\text{MnO}_3$ (where Re is a rare-earth element (La, Nd, ...) and A is an alkaline-earth metal (Sr, Ca, ...)) differ substantially from the properties of the corresponding bulk single crystals. This difference is mainly caused by the mechanical stresses in a film induced by the misfit between the film and substrate. The magnetic anisotropy induced by this mechanism will be called magnetocrystalline anisotropy, in contrast to crystalline anisotropy, which is induced by the crystal structure of a substance and, hence, is characteristic of bulk samples. The magnetic properties of films also depend substantially on the effects of phase separation and a nonstoichiometric composition and the presence of a nonmagnetic layer on the substrate–film interface (which is important only for a film thickness smaller than 10 nm [11]). Moreover, these effects depend on the manganite film composition, the preparation method, and the substrate material. The magnetic properties of thin $\text{La}_{1-x}\text{Sr}_x\text{MnO}_3$ manganite films (in most works, $\text{La}_{0.7}\text{Sr}_{0.3}\text{MnO}_3$; hereafter, LSMO) were usually studied in the (001) LSMO orientation. The films were grown on (001) SrTiO_3 (STO), (001) LaAlO_3 (LAO), (001)[$(\text{LaAlO}_3)_{0.3} + (\text{Sr}_2\text{AlTaO}_6)_{0.7}$] (LSAT), (110) NdGaO_3 (NGO), and so on [1–10].

The authors of [3, 12–14] found that, apart from the cubic magnetic anisotropy induced by the crystal structure of LSMO, these films exhibit a uniaxial in-plane magnetic anisotropy, which is significantly stronger than the crystalline anisotropy in some cases.

The uniaxial anisotropy was assumed to be caused by the misfit between the lattice parameters of the film and substrate materials.

The growth and magnetic properties of epitaxial LSMO films was studied in [14] for the basic (110), (001), (100), and (010) orientations of an NGO substrate. For all NGO substrate orientations, a uniaxial magnetic anisotropy was detected in the substrate plane, which was also explained by misfit-induced stresses in a film. In [12], a uniaxial in-plane anisotropy was observed at liquid-nitrogen temperatures in LSMO films deposited onto an STO substrate in which the (001) plane was tilted at an angle of 10°. The investigation of LSMO films deposited onto (001) STO substrates in which the (001) plane was tilted at low angles (0.13°, 0.24°) to the normal to the substrate surface demonstrated a uniaxial anisotropy in the substrate plane at room temperature and a predominant biaxial anisotropy at lower temperatures (about 100 K) [15]. A detailed examination in the temperature range 20–300 K of LSMO films deposited onto (001) STO, (001) MgO, (001) LAO, etc., substrates revealed that the crystalline anisotropy decreased strongly with increasing temperature at a retained contribution of uniaxial anisotropy in the films [3].

Thus, although the magnetic anisotropy in LSMO films has been studied in many works, the coexistence of their crystalline anisotropy and the strain-induced uniaxial anisotropy is still unclear. The purpose of this work is to quantitatively estimate the magnetic anisotropy of an epitaxial LSMO film under conditions of a controlled lattice misfit between the film and substrate

Table 1. Tilt angles β , lattice parameters a_{\perp} , and rocking curve widths Δ_{ω} of some LSMO films deposited onto tilted NGO substrates and (001)STO and (001)LSAT substrates

Substrate orientation	β	a_{\perp} , nm	Δ_{ω}
(110)NGO	0	0.3904	0.037°
(450)NGO	6°	0.3904	0.04°
(230)NGO	10.9°	0.3916	0.08°
(130)NGO	25.7°	0.3912	0.08°
(120)NGO	18.7°	0.3913	0.05°
(001)STO	0	0.3845	0.014°
(001)LSAT	0	0.3875	0.06°

materials. The other film parameters were maintained at the same level. To solve this problem, we studied the magnetic anisotropy of epitaxial $\text{La}_{0.7}\text{Sr}_{0.3}\text{MnO}_3$ films deposited onto NGO substrates in which the (110) plane was tilted to the substrate plane. By controlling this tilt angle, we changed the lattice misfit between the substrate and film, which was measured experimentally. To study the magnetic anisotropy at room temperature, we used the following three independent methods: an investigation of magnetization using the magneto-optical Kerr effect, an analysis of ferromagnetic resonance (FMR) spectra at a frequency of 9.61 GHz, and recording of absorption spectra of electromagnetic radiation at a frequency of 290.6 MHz.

2. EXPERIMENTAL

Epitaxial LSMO films 40–100 nm thick were deposited by laser ablation (KrF laser, $\lambda = 248$ nm) at a temperature of 600–800°C and an oxygen pressure of 0.2 mbar. Most films were deposited onto neodymium gallate (NGO) substrates whose (110) plane was rotated about the [001] direction at angle β falling in the range 0–26°. As a result, the substrate surface coincided with the crystallographic planes given in Table 1. We also studied several LSMO films deposited onto (001)LSAT and (001)STO substrates in order to illustrate the anisotropy effects caused by a change in the substrate material. The crystallographic parameters of the films and substrates were determined on a Philips X-ray diffractometer by measuring X-ray diffraction patterns under conditions where both incident and reflected X-ray beams lied in a plane normal to the (110)NGO plane [10].

Table 1 gives the lattice parameters in the [001] direction for LSMO films deposited onto NGO substrates in which the (110) plane is tilted at an angle $\beta = 0$ –25.7° to the interface about the [001]NGO direction. Rocking curve widths Δ_{ω} are also given in Table 1. For comparison, Table 1 also contains the parameters of LSMO films deposited onto STO and LSAT substrates. The grown LSMO films were strictly oriented

with respect to both the normal to the (110)NGO plane of the substrate and a preferred direction in the substrate plane. Lattice parameter a_{\perp} in the LSMO films along the normal to the (110) plane of the NGO substrate was determined from X-ray diffraction patterns recorded in a scanning mode. We supposed that the LSMO films had a crystal structure close to the structure of cubic perovskite (see, e.g., review [2]). The small rhombohedral or orthorhombic distortions caused by the lattice misfit between the film and substrate materials were taken into account in the magnetic parameters of the films.

As follows from Table 1, the quality of all films is rather high: in all cases, $\Delta_{\omega} < 0.1^\circ$. It is seen that, as the tilt angle of the substrate increases, lattice parameter

a_{\perp} of a film in the $[\bar{1}10]$ NGO direction increases (except for a film with $\beta = 10.9^\circ$). This behavior is usually observed when the LSMO lattice is compressed in the basal plane [1, 2, 10]. The best correspondence of the unit cell size in the pseudo-cubic representation ($a_{\text{LSMO}} = 0.3876$ nm) obtained from the measurements of LSMO polycrystals [16] was observed on LSAT substrates having the minimum lattice misfit between the substrate and film. On the whole, we can conclude that the grown magnetic films are subjected to the mechanical stresses induced by their interaction with the substrates. These stresses provide compressive forces for NGO and tensile forces for STO and LSAT.

The presence of a ferromagnetic phase in the LSMO films at room temperature makes it possible to investigate the magnetic parameters with the use of the magneto-optical Kerr effect without additional cooling, which simplifies the measurements of the spatial anisotropy of the magnetic parameters. This technique was described in detail in [10]. As a result, we measured the angular dependences of magnetization curves, which was used to determine the directions of easy and hard magnetization axes and saturation field H_s for a magnetic field applied along the hard axis. The value of field H_s determined under these conditions was taken to be the anisotropy field.

FMR spectra were recorded at room temperature and studied at a frequency of 9.61 GHz on a standard Bruker ER 200 magnetic resonance spectrometer operating in the microwave range [10]. We analyzed the angular dependence of the FMR field under conditions where a dc magnetic field and the magnetic component of a radio-frequency field were perpendicular to each other and retained in the film plane during rotation (so-called parallel orientation). Rotation was performed about the axis normal to the film plane. This technique excludes a change in the signal shape due to shape anisotropy and makes it possible to investigate in-plane anisotropy alone. The FMR field is related to the irradiation frequency through a certain relationship, which contains the magnetization and the anisotropy fields of various symmetries as parameters. With this resonance technique, we were able to

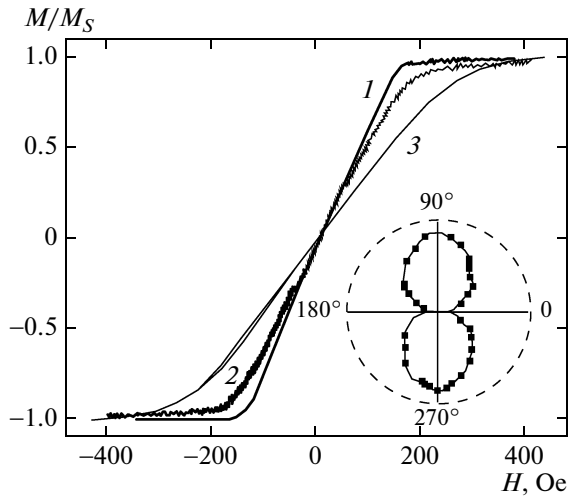


Fig. 1. Magnetization curves of LSMO/NGO films with various angles of (110)NGO plane tilt β recorded when a magnetic field is applied along a hard magnetization axis: $\beta = (1)$ 6.0° , (2) 18.7° , and (3) 25.7° . (inset) Angular dependence of the saturation field for a sample with $\beta = 6.0^\circ$ presented in the polar coordinates.

substantially increase the accuracy of determining the anisotropy parameters.

The radio-frequency absorption at room temperature and a frequency of 290.6 MHz was studied with a unique magnetic resonance spectrometer based on a Q meter [17] also under parallel orientation conditions. The applied magnetic field was varied in the range 0–800 Oe, and it was modulated by an additional ac magnetic field at a frequency of 47 kHz and an amplitude of 0–5 Oe. We recorded the first harmonic of an absorption signal in the course of synchronous detection at the modulation frequency of an applied magnetic field during a change in it. As will be shown below, this technique allowed us to measure the uniaxial anisotropy in the grown LSMO films.

3. EXPERIMENTAL RESULTS

Figure 1 shows the magnetization curves of the LSMO films grown on NGO substrates having various tilt angles of the (110)NGO crystallographic plane. These curves were recorded at room temperature using the magneto-optical Kerr effect. With these curves, we determined saturation field H_s as the abscissa corresponding to the maximum curvature of a magnetization curve. The inset to Fig. 1 shows an example of the angular dependence of the saturation field. These curves clearly demonstrate the presence of a uniaxial anisotropy in the LSMO/NGO films. Segments 0–180° and 90°–270° in the inset indicate the easy and hard magnetization axis directions, respectively. In all films deposited onto (110) substrates, the easy axis is determined by the $[1\bar{1}0]$ direction of the substrate.

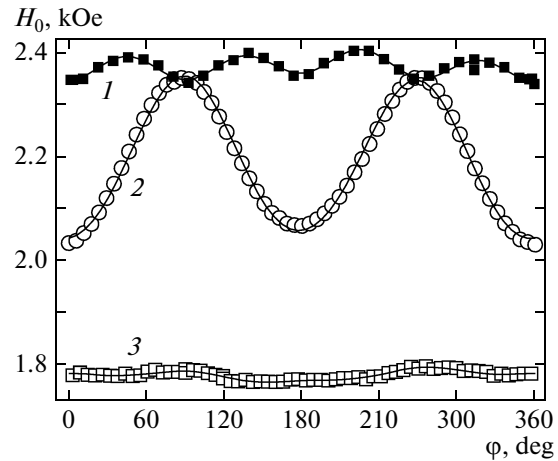


Fig. 2. Angular dependences of the resonance field of FMR lines for (1) LSMO/LSAT, (2) LSMO/NGO, and (3) LSMO/STO films recorded at room temperature and a frequency of 9.61 GHz: (symbols) experimental data and (solid curves) calculation by Eq. (4).

Moreover, we will show below that the values of saturation field H_s obtained from the magnetization curves when an applied field is directed along the hard axis can also be used to determine the field of a uniaxial in-plane anisotropy. As follows from the curves shown in Fig. 1, the saturation field increases with the tilt angle of the (110)NGO plane. It should be noted that the uncertainty in determining H_s also increases with β . Nevertheless, with this technique, we can qualitatively estimate the variation of H_s with angle β .

We now present our experimental data obtained by magnetoresonance spectroscopy at room temperature. First of all, note that, with FMR, we detected the crystalline magnetic anisotropy induced by the cubic structure of LSMO in all LSMO films grown on all substrates. Figure 2 shows an example of the angular dependence of the resonance field of the FMR line of manganese ions that was recorded at a frequency of 9.61 GHz for LSMO films deposited onto NGO, LSAT, and STO substrates. Recall that a sample was rotated about the normal to a film and a dc magnetic field and the magnetic component of a radio-frequency field lied in the film plane during rotation. Angle of rotation ϕ was measured from the $[1\bar{1}0]$ NGO direction, which specifies an easy magnetization axis. It is clearly visible that the contribution of uniaxial anisotropy in the case of LSMO/NGO (see circles in Fig. 2) is substantially larger than the contribution of the cubic anisotropy inherent in an LSMO single crystal. In this case, angles of 0 and 180° correspond to an easy magnetization axis and angles of 90° and 270° correspond to a hard magnetization axis. In two other cases, a uniaxial anisotropy is not so pronounced; nevertheless, the processing of the experi-

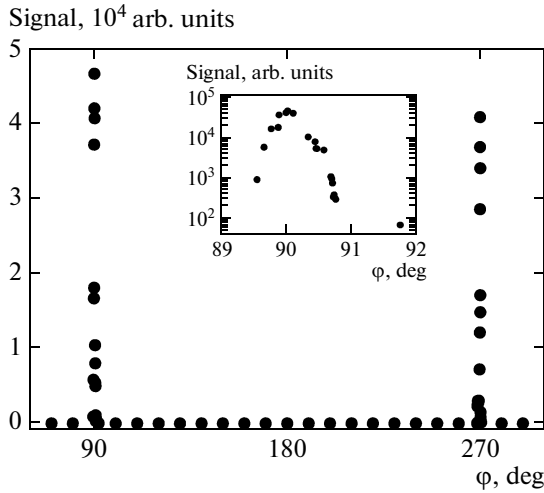


Fig. 3. Angular dependence of the absorption signal amplitude at a frequency of 290.6 MHz. (inset) Signal shape in the hard axis region.

mental data also supports its presence in the corresponding films.

The searching for FMR spectra at a frequency of 290.6 MHz in the magnetic field range 0–800 Oe did not give positive results. FMR lines were detected for some samples in very narrow angular ranges, and we will not dwell on them. The giant absorption signals detected for all LSMO/NGO samples are thought to be of great interest. Figure 3 shows the angular dependence of such a signal recorded at a frequency of 290.6 MHz. Absorption is seen to appear only when an applied magnetic field is oriented along the hard magnetization axis. The signal demonstrates resonance behavior in a change in both the magnetic field and the angle of rotation. It should be noted that the signal amplitude changes several orders of magnitude in a very narrow angular range, 1° – 5° , depending on the sample. In Fig. 3, this dependence becomes an almost vertical line; therefore, it is shown in more detail in the inset. The detection of this signal determines the direction of the hard magnetization axis at a high accuracy, and (as will be shown below) the magnetic field at which this signal appears corresponds to the uniaxial anisotropy field.

4. DISCUSSION OF RESULTS

To interpret our experimental data, we use the following relationship for the free energy density in an LSMO film:

$$F = -\mathbf{M} \cdot \mathbf{H} - \frac{K_u}{M^2} (\mathbf{M} \cdot \mathbf{n}_u)^2 + \frac{1}{2} (\mathbf{M} \cdot \hat{N}^c \mathbf{M}) + 2\pi (\mathbf{M} \cdot \mathbf{e}_z)^2. \quad (1)$$

Here, \mathbf{M} is the magnetic moment vector, \mathbf{H} is the applied magnetic field, K_u is the uniaxial anisotropy constant, \mathbf{n}_u is the unit vector directed along the easy

magnetization axis, \hat{N}^c is the crystalline anisotropy tensor, and \mathbf{e}_z is the unit vector along the z axis. The coordinate system is chosen so that the x axis coincides with the direction of dc applied magnetic field \mathbf{H}_0 and the z axis is normal to the film. The first term in Eq. (1) describes the Zeeman energy; the second, the uniaxial anisotropy energy; the third, the crystalline anisotropy; and the last, the anisotropy induced by the sample shape.

To estimate the uniaxial anisotropy field (which was calculated by the standard formula $H_u = 2K_u/M$), we used the saturation fields determined in the experiments on measuring the magnetization when an applied magnetic field was directed along the hard magnetization axis. Indeed, if we restrict ourselves to the first two terms in Eq. (1), the condition of the minimum free energy density for an applied magnetic field directed along the hard magnetization axis leads to the following relationship for equilibrium angle φ_M at which the magnetic moment is directed with respect to the x axis and, hence, the applied magnetic field:

$$\cos \varphi_M = H/H_u.$$

This means that the equilibrium magnetic moment at $H = H_u$ is directed along an applied magnetic field and, hence, along the hard magnetization axis, and its value is equal to saturation magnetization M_s in the single-domain ferromagnet approximation. Therefore, with the curves shown in Fig. 1, we can determine the fields at which the magnetization is saturated and to attribute these fields to the uniaxial anisotropy fields. The uniaxial anisotropy fields thus found are shown as triangles in Fig. 4, and the errors, which are fully determined by the errors in determining H_s , are also shown there. The anisotropy fields obtained using the magneto-optical Kerr effect are seen to correctly describe the real situation.

The study of FMR spectra gives much more accurate values of the magnetic parameters of a substance. To analyze the angular dependence of a spectrum, we use the Landau–Lifshitz equation, which describes the precessional motion of magnetic moment \mathbf{M} under the action of dc magnetic field \mathbf{H}_0 and the magnetic component of radio-frequency field \mathbf{h} ,

$$\dot{\mathbf{M}} = -\gamma \mathbf{M} \times \mathbf{H}_{\text{eff}}. \quad (2)$$

Here, effective magnetic field \mathbf{H}_{eff} is determined by the relationship $\mathbf{H}_{\text{eff}} = -\delta F/\delta \mathbf{M}$, and the magnetic field for F in Eq. (1) is $\mathbf{H} = \mathbf{H}_0 + \mathbf{h}$. We do not write the relaxation term in the right-hand side of Eq. (2), since we are only interested in a change in the resonance field, which is independent of decay processes. For the chosen spatial orientation of a film, the expressions for the nonzero tensor \hat{N}^c components with allowance for

only the first term in the expansion of the crystalline anisotropy energy have the form [18]

$$\begin{aligned} N_{xx}^c &= \frac{K_1}{M_0^2} (2 - \sin^2 2\varphi_c), \\ N_{yy}^c &= \frac{3K_1}{M_0^2} \sin^2 2\varphi_c, \end{aligned} \quad (3)$$

where K_1 is the crystalline anisotropy constant and φ_c is the angle at which the crystalline anisotropy axis is directed with respect to the x axis. We now use the standard procedure [18, 19] to solve a linearized Landau – Lifshitz equation for high-frequency magnetization $\mathbf{m} = \mathbf{M} - \mathbf{M}_0$ (where \mathbf{M}_0 is the equilibrium magnetization), which is sought for in the form $\mathbf{m}(t) = \mathbf{m} \exp(-i\omega t)$. As a result, we obtain the resonance relationship [19]

$$\begin{aligned} \left(\frac{\omega}{\gamma}\right)^2 &= \left(4\pi M_0 + H_0 + H_u \cos^2 \varphi_u + H_c \frac{1 + \cos^2 2\varphi_c}{2}\right) \\ &\times (H_0 + H_u \cos 2\varphi_u + H_c \cos 4\varphi_c), \end{aligned} \quad (4)$$

where ω is the cyclic frequency of the radio-frequency field, γ is the gyromagnetic ratio, φ_u is the angle at which the easy axis of uniaxial anisotropy is directed with respect to the x axis, $H_c = 2K_c/M_0$ is the cubic anisotropy field, and K_c is the cubic anisotropy constant. As a rule, magnetic spectroscopy uses a stabilized electromagnetic irradiation frequency, and an absorption spectrum is recorded in the course of variation of an applied magnetic field. Therefore, using Eq. (4), we should obtain an explicit dependence of resonance field H_0 on angles φ_u and φ_c . We will not write down this awkward expression. However, it should be noted that, apart from uniaxial and cubic anisotropy, the LSMO/NGO films have an anisotropic contribution with a period of 360° (the minimum in the dependence for LSMO/NGO in Fig. 2 at 180° is noticeably higher than the minima at 0 and 360°). This contribution can be explained by the nonequivalence of the film surfaces: the surface at the interface with the substrate undergoes a stronger effect of the substrate than the external surface does. As a result, we take into account this contribution in a phenomeno-

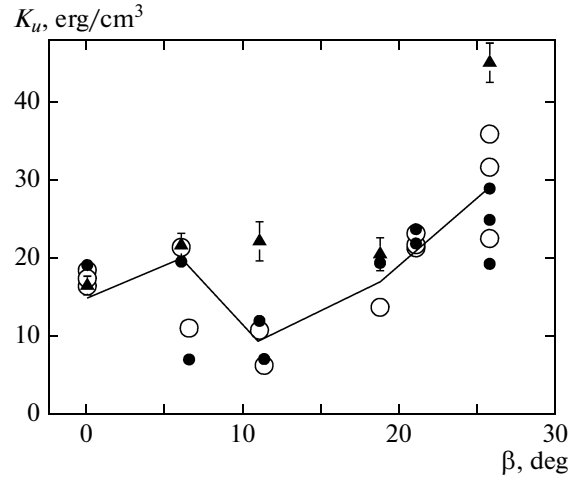


Fig. 4. Uniaxial anisotropy constant vs. the tilt angle of the (110)NGO substrate plane: (▲) magneto-optical Kerr effect, (○) FMR at a frequency of 9.61 GHz, and (●) absorption at a frequency of 290.6 MHz. (broken line) Calculation by Eq. (10) with the parameters from Table 1.

logical manner, by adding the term $H_s \cos \varphi_s$ to the expression for the resonance field obtained by solving quadratic equation (4).

From an experiment, we obtain the dependence of resonance field H_0 on angle of film plane rotation φ . This angle is connected to angles φ_u , φ_c , and φ_s by the following relations:

$$\varphi_u = \varphi + \psi_1, \quad \varphi_c = \varphi + \psi_2, \quad \varphi_s = \varphi + \psi_3.$$

We are interested in anisotropy fields H_u , H_c , and H_s , equilibrium magnetization M_0 , and the angles of rotation of easy axes with respect to each other (i.e., the differences $\Delta\varphi_c = \varphi_c - \varphi_u$ and $\Delta\varphi_s = \varphi_s - \varphi_u$). Table 2 gives the parameters of several LSMO/NGO samples at seven tilt angles of a substrate that were obtained by processing our FMR angular experiments. It should be noted that the high sensitivity of FMR allowed us to determine parameters M_0 , H_u , H_c , and $\Delta\varphi_c$ at root-mean-square errors of several percent.

It is seen from Table 2 that all films have an anisotropy field induced by the cubic structure of LSMO; however, this biaxial anisotropy is at least an order of

Table 2. Magnetic anisotropy parameters

β	M_0 , Oe	H_u , Oe	H_c , Oe	H_s , Oe	$\Delta\varphi_c$	K_u , kerg/cm ³	K_1 , kerg/cm ³
0	331	105	13.6	1.5	45.7°	17.5	2.25
6.0°	280	153	14	16	42.5°	21.4	1.96
6.5°	178	125	10.4	31.7	45.6°	11.1	0.93
11.0°	254	86	6.7	9.8	45.0°	10.9	0.85
18.7°	226	122	15	14	46.0°	13.8	1.70
21.0°	295	158	14.9	1.4	43.6°	23.2	2.20
25.7°	322	197	20	20	43.6°	31.7	3.22

magnitude lower than the uniaxial anisotropy induced by the additional strained state of a film. The angles of rotation of the easy axes of these two types of anisotropy are close to 45° , which is explained by the substrate orientation, where one of the substrate faces is oriented parallel to the [001]NGO direction, which specifies a hard magnetization axis and coincides with the crystallographic [001]LSMO axis [13, 14].

Figure 4 shows the experimental values of uniaxial anisotropy constant K_u for LSMO films with various tilt angles β of the (110)NGO substrate plane. The anisotropy constants were calculated by the formula $K_u = H_u M/2$ using the values of H_u determined independently using the following three types of experiments: the study of the magnetic parameters using the magneto-optical Kerr effect, the processing of the angular dependences of FMR spectra at a frequency of 9.61 GHz, and the correspondence between the resonance fields of giant absorption signals at a frequency of 290.6 MHz and the uniaxial anisotropy fields.

The last statement can be elucidated by the following consideration. The authors of [20, 21] showed that the field dependence of the static magnetic susceptibility of uniaxial ferromagnetic films has a sharp peak near anisotropy field H_u when an applied magnetic field is directed along the hard magnetization axis. This peak follows from the solution to the Landau–Lifshitz equation with a free energy in the form of (1) without regard for cubic anisotropy, as was done in [20, 21]. However, it can also be obtained simply from the condition of the minimum free energy, which yields the field dependence of the angle of the magnetization vector with respect to the applied magnetic field. The field derivative of this dependence has a sharp peak near the anisotropy field, which, in turn, causes a peak of static magnetic susceptibility that is normal to the applied field. In experiments on magnetic resonance, the imaginary part of a dynamic susceptibility is measured, and its general form can be written as $\chi''(\omega\tau) = \chi_0 f(\omega\tau)$, where $f(\omega\tau)$ is a certain function of rate τ^{-1} of the relaxation process that determines magnetization decay. Thus, the described absorption signal can be used to obtain information on relaxation mechanisms; however, this is beyond the scope of this work.

It is seen in Fig. 4 that the use of the magneto-optical Kerr effect for determining the uniaxial anisotropy constants (triangles in Fig. 4) led to substantial deviations from both the results obtained by other techniques and the calculated results in some cases. These deviations are thought to be caused by the fact that, first, the single-domain approximation can be violated for some samples and, second, taking into account only uniaxial anisotropy can be insufficient [12].

We now discuss the physical basis of the induced uniaxial anisotropy in the LSMO/NGO films. We already noted the works of other scientific teams dealing with the anisotropy of LSMO films on tilted sub-

strates [12, 15]. However, those authors only studied LSMO films on SrTiO₃ and, which is most important, did not propose a grounded mechanism for the appearance of a uniaxial anisotropy. The authors of [22, 23] investigated the anisotropy of epitaxial iron films grown on tilted silver substrates with a tilt angle of 0 – 14° . In those works, the magneto-optical Kerr effect was used to show that the uniaxial anisotropy increases with the tilt angle according to a quadratic law. However, they noted that the nature of this anisotropy was still unclear. Moreover, they assumed that the uniaxial anisotropy can be induced by additional stresses in the direction normal to the film plane, which, in turn, are caused by the lattice misfit of the substrate and film.

Let us consider how the film anisotropy is related to the interactions of crystalline sites that undergo the additional mechanical stresses induced by the difference from the lattice constants of the substrate. To this end, we write the following expression for the free energy density of a ferromagnetic sample without regard for the formation of a domain structure at a tilted epitaxial film growth plane and using no assumptions regarding the character of anisotropy [24]:

$$F = -\mathbf{M} \cdot \mathbf{H} + \frac{1}{2}(\mathbf{M} \cdot \hat{N}\mathbf{M}) + F_{mc}. \quad (5)$$

Here, the first term describes the Zeeman energy, the second term describes the shape anisotropy energy with demagnetizing tensor \hat{N} , and the last term describes the energy caused by both the crystal structure of the substance and the additional stresses appearing in the crystal lattice due to various factors. For the case of a thin film, the expression for the shape anisotropy can be simplified to the form

$$\frac{1}{2}(\mathbf{M} \cdot \hat{N}\mathbf{M}) = \frac{1}{2}M^2 \cos^2 \alpha_z, \quad (6)$$

where $\cos^2 \alpha_z$ is the direction cosine of the magnetization vector with respect to the z axis directed normal to the film plane.

When the cubic symmetry of a crystal structure, in particular, an epitaxial LSMO film grown on an orthorhombic neodymium gallate substrate, is violated, for F_{mc} we can write

$$F_{mc} = K_x \cos^2 \alpha_x + K_y \cos^2 \alpha_y + K_z \cos^2 \alpha_z, \quad (7)$$

where $K_{x,y,z}$ are magnetocrystalline anisotropy constants and $\cos \alpha_{x,y,z}$ are the direction cosines of the magnetization vector with respect to the crystallographic axes. If the crystal structure is tilted at angle β to the film plane about axis x , we can rewrite Eq. (5) in the form

$$\begin{aligned}
F = & -\mathbf{M} \cdot \mathbf{H} + \frac{1}{2} M^2 \cos^2 \alpha_z + K_x \cos^2 \alpha_x \\
& + K_y (\cos \beta \cos \alpha_z - \sin \beta \cos \alpha_x)^2 \\
& + K_z (\sin \beta \cos \alpha_x + \cos \beta \cos \alpha_z)^2
\end{aligned} \quad (8)$$

after passing from the coordinate system related to the crystal structure (x' , y' , z') to the coordinate system related to the film plane (x , y , z).

When considering the rotation of the magnetization vector in the film plane, we assume $\alpha_z = \pi/2$. Since $\cos^2 \alpha_x + \cos^2 \alpha_y = 1$ in this case, we can reduce Eq. (8) to the form

$$\begin{aligned}
F = & -\mathbf{M} \cdot \mathbf{H} \\
& + [K_x - K_y + (K_y - K_z) \sin^2 \beta] \cos^2 \alpha_x,
\end{aligned} \quad (9)$$

which corresponds to the problem of a uniaxial magnetic anisotropy with the anisotropy constant

$$K_u = K_x - K_y + (K_y - K_z) \sin^2 \beta. \quad (10)$$

Note that this expression well describes the experimental data on the angular dependence of the anisotropy of iron films deposited onto silver substrates having various tilt angles [22, 23].

Figure 4 shows the broken line calculated by Eq. (10) using three fitting parameters, K_x , K_y , and K_z . Note that, when angle β increases, the contribution to magnetocrystalline anisotropy K_u in the [001]LSMO direction for the films grown epitaxially on a (110)NGO substrate dominates over those of other directions. Therefore, we assumed that anisotropy constants K_x and K_y are independent of angle β and that constant K_z is proportional to the squared crystalline strain along the [001]LSMO direction. The strain was determined as the difference between the experimental values of a_{\perp} taken from Table 1 and the lattice parameter of LSMO in the quasi-cubic approximation ($a_L = 0.3876$ nm [2]) using the relation $2(a_{\perp} - a_L)/(a_{\perp} + a_L)$. It is seen that the broken line in Fig. 4 well describes the experimental points; hence, analytical Eq. (10) satisfactorily reflects the real situation.

5. CONCLUSIONS

We studied the in-plane magnetic anisotropy of epitaxial $\text{La}_{0.7}\text{Sr}_{0.3}\text{MnO}_3$ films at room temperature as a function of the lattice misfit between the films and various substrates. We rotated the (110) NdGaO_3 plane of the substrate in order to change the state of stress in the crystal structure of LSMO in the direction normal to the plane in a controlled manner, retaining all other film parameters unchanged. We analyzed the films using the following three independent techniques: magneto-optical Kerr effect, ferromagnetic resonance at a frequency of 9.61 GHz, and recording of absorption spectra of electromagnetic radiation at a frequency of 290.6 MHz. As a result, we obtained an experimental dependence of in-plane uniaxial anisotropy

on the lattice misfit between a film and the substrate. We proposed a physical model to describe the change in the magnetic anisotropy induced by a change in the lattice misfit between a film and the substrate. The calculations performed with this model satisfactorily describe the experimental results. The anisotropy parameters of the LSMO films grown on (001) NdGaO_3 , (001) SrTiO_3 , and (001)[$(\text{LaAlO}_3)_{0.3} + (\text{Sr}_2\text{AlTaO}_6)_{0.7}$] substrates were compared. A sharp increase in the radio-frequency absorption in a narrow angular range of a dc magnetic field near a hard magnetization axis was detected. This resonance effect makes it possible to measure the anisotropy field directly.

ACKNOWLEDGMENTS

We thank V.A. Atsarkin, Yu.A. Boikov, D. Winkler, A.L. Vlasyuk, T. Claeson, K.I. Constantinyan, I.M. Kotelyanskii, Ya.M. Mukovskii, and A.V. Shchadrin for helpful discussions of the results and for assistance in performing the investigations.

This study was supported in part by the programs of the Department of Physical Sciences and the Presidium of the Russian Academy of Sciences, Ministry of Education and Science of the Russian Federation (project no. 02.740.11.0795), the President of the Russian Federation in terms of the program for Support of Leading Scientific Schools (grant no. NSh-5408.2008.2), the Russian Foundation for Basic Research (project nos. 08-02-00487, 08-02-00040), and the International Center of Science and Technology (grant no. 3743).

REFERENCES

1. W. Prellier, Ph. Lecoeur, and B. Mercey, *J. Phys: Condens. Matter* **13**, R915 (2001).
2. A.-M. Haghiri-Cosnet and J. P. Renard, *J. Phys. D: Appl. Phys.* **36**, R127 (2003).
3. K. Steenbeck and R. Hiergeist, *Appl. Phys. Lett.* **75**, 1778 (1999).
4. M. Ziese, H. S. Semmelhack, and P. Busch, *J. Magn. Magn. Mater.* **246**, 327 (2002).
5. P. Dey, T. K. Nath, and A. Tarapher, *Appl. Phys. Lett.* **91**, 012511 (2007).
6. F. Tsui, M. C. Smoak, T. K. Nath, and C. B. Eom, *Appl. Phys. Lett.* **76**, 2421 (2000).
7. Y. P. Lee, S. Y. Park, Y. H. Hyun, J. B. Kim, V. G. Prokhorov, V. A. Komashko, and V. L. Svetchnikov, *Phys. Rev. B: Condens. Matter* **73**, 224413 (2006).
8. Yan Wu, Y. Suzuki, U. Rüdiger, J. Yu, A. D. Kent, T. K. Nath, and C. B. Eom, *Appl. Phys. Lett.* **75**, 2295 (1999).
9. Y. Suzuki, H. Y. Hwang, S.-W. Cheong, T. Siegrist, R. B. van Dover, A. Asamitsu, and Y. Tokura, *J. Appl. Phys.* **83**, 7064 (1998).
10. G. A. Ovsyannikov, A. M. Petrzhik, I. V. Borisenko, A. A. Klimov, Yu. A. Ignatov, V. V. Demidov, and

- S. A. Nikitov, Zh. Eksp. Teor. Fiz. **135** (1), 56 (2009) [JETP **108** (1), 48 (2009)].
11. M. Bibes, S. Valencia, L. Balcells, B. Martinez, J. Fontcuberta, M. Wojcik, S. Nadolski, and E. Jedryka, Phys. Rev. B: Condens. Matter **66**, 134416 (2002).
 12. Z.-H. Wang, G. Cristiani, and H.-U. Habermeire, Appl. Phys. Lett. **82**, 3731 (2003).
 13. M. Mathews, R. Jansen, G. Rijnders, J. C. Lodder, and D. H. A. Blank, Phys. Rev. B: Condens. Matter **80**, 064408 (2009).
 14. H. Boschker, M. Mathews, E. P. Houwman, H. Nishikawa, A. Vailionis, G. Koster, G. Rijnders, and D. H. A. Blank, Phys. Rev. B: Condens. Matter **79**, 214425 (2009).
 15. M. Mathews, F. M. Postma, J. C. Lodder, R. Jansen, G. Rijnders, and D. H. A. Blank, Appl. Phys. Lett. **87**, 242507 (2005).
 16. M. C. Martin, G. Shirane, Y. Endoh, K. Hirota, Y. Moritomo, and Y. Tokura, Phys. Rev. B: Condens. Matter **53**, 14285 (1996).
 17. A. E. Mefed and V. V. Demidov, Prib. Tekh. Eksp., No. 3, 99 (2008) [Instrum. Exp. Tech. **51** (3), 418 (2008)].
 18. A. G. Gurevich, *Magnetic Resonance in Ferrites and Antiferromagnets* (Nauka, Moscow, 1973) [in Russian].
 19. T. M. Vasilevskaya and D. I. Sementsov, Fiz. Met. Metalloved. **108** (4), 339 (2009) [Phys. Met. Metallogr. **108** (4), 321 (2009)].
 20. B. A. Belyaev, A. V. Izotov, and S. Ya. Kiparisov, Pis'ma Zh. Eksp. Teor. Fiz. **74** (4), 248 (2001) [JETP Lett. **74** (4), 226 (2001)].
 21. T. M. Vasilevskaya and D. I. Sementsov, Zh. Eksp. Teor. Fiz. **137** (5), 861 (2010) [JETP **110** (5), 754 (2010)].
 22. R. K. Kawakami, E. J. Escorcia-Aparicio, and Z. Q. Qui, Phys. Rev. Lett. **77**, 2570 (1996).
 23. Y. Z. Wu, C. Won, and Z. Q. Qui, Phys. Rev. B: Condens. Matter **65**, 184419 (2002).
 24. S. V. Vonsovskii, *Magnetism* (Nauka, Moscow, 1971; Wiley, New York, 1974).

Translated by K. Shakhlevich